Supporting Information

Remarkable energy barrier for spin reversal in field induced dinuclear ytterbium single molecule magnet

Arpan Mondal and Sanjit Konar*

Department of Chemistry, Indian Institute of Science Education and Research (IISER), Bhopal By-pass Road, Bhauri, Bhopal-462066, India

Experimental Section:

As received analytical grade chemicals and reagents were used from commercial sources without further purification. All the reactions were carried under aerobic conditions. The metal salts [$Yb(NO)_3$], picolinaldehyde, 2-hydroxy-5-methylbenzaldehyde, and triethylamine were purchased from Sigma Aldrich Chemical Co. The Powder X-ray diffraction (PXRD) data for the compound was collected on a PANalytical EMPYREAN instrument using Cu-Kα radiation. The Elementar Microvario Cube Elemental Analyzer was used for elemental analyses. IR spectrum was recorded on KBr pellets by Perkin-Elmer spectrometer. The ^{1}HNMR spectrum was collected in Bruker's AVANCE-III 500MHz NMR spectrometers. The magnetic susceptibility measurements were carried out with a Quantum Design SQUID-VSM magnetometer for both the samples. The sample holder correction was done for the experimentally measured values and and the diamagnetic correction was estimated by Pascal's constants[1] for the studied compound.

Crystal Data Collection and Structure Determination:

A Brüker APEX-II CCD diffractometer with a graphite monochromated Mo-Kα radiation (α = 0.71073 Å) was used to collect the X-ray data for complex **1**. the data collection was performed with the φ and ω scan and solved using direct methods followed by full-matrix least square refinements against F^2 (all data HKLF 4 format) using SHELXTL.[2] The structure was solved in the Olex2[3] software interface using intrinsic phasing in ShelXT structure solution proggrame. The positions of the non-hydrogen atoms were confirmed by the subsequent difference Fourier synthesis and least-square refinement. All the non-hydrogen atoms were refined anisotropically and hydrogen atoms were placed geometrically and refined using the riding model. The crystallographic details for complexes **1** have been summarized in Table S1 and CCDC 2044800 contain the crytal data for this paper. These data can be obtained free of charge from the Cambridge Crystallographic Data Centre via www.ccdc.cam.ac.uk/data_requested/cif.

Computational Details:

All the calculations were performed on the coordinates obtained from the single crystal structure without optimization using MOLCAS 8.2 software package.[4] On the other hand, for model complex **1a**, we fixed the water molecules in the axial position at an average distance 2.30 Å according to the other reported Yb complexes. Then the hydrogen optimization was performed with the corresponding Gd-complex and the optimized coordinates were used for further calculations. The ab initio calculations were performed on trivalent Yb centre and the single ion anisotropy was calculated by replacing the paramagnetic lanthanide ion with diamagnetic Lu^{+3} ion. We employed the basis set from ANO-RCC library for all the calculations e.g ANO-

RCC...9s8p6d4f3g2h. for Yb and Lu, ANO-RCC...3s2p1d for O and N, ANO-RCC...3s2p., for C and ANO-RCC...2s. for H. In addition, the Douglas-Kroll-Hess Hamiltonian[5] has been used to include the relativistic effect. To obtain the energy of the spin-free eigen states we have performed the complete active space self-consistence field (CASSCF) method[6] by including 13 electrons in 7 4f orbitals for Yb^{III} ion. In this active space 7 doublets excited states have been consider in the configuration interaction procedure to compute the magnetic anisotropy of the single metal centers. Also we used RASSI-SO[7] to introduce the spin-orbit coupling within the space of the calculated spin-free eigen states for both compounds. Further to compute the g tensor and the crystal field parameters we have used the Single_Aniso module[8] as implemented in MOLCAS by considering previously calculated spin-orbit sates. In addition, the Cholesky decomposition for 2-eletron integrals was used throughout the calculations to save the disk space.

Synthesis of Picolinohydrazide: The picolinohydrazide was synthesized by the simple condensation reaction between picolinaldehyde (5 mmol, 0.475 ml) and excess hydrazine hydrate (50 mmol, 2.5 ml) in MeOH solvent (~25 ml) at 80 ºC for 24 h. A white color microcrystalline precipitate was obtained (Yield 80%) and wash with cold methanol and used further without purification.

^{1}H NMR for Picolinohydrazide

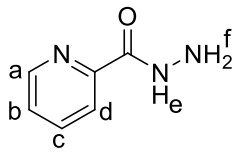

^{1}H NMR (500 MHz, DMSO-d_6): δ_H 9.896 (s, H_e), 8.599 (d, H_a), 7.93-8.00 (m, H_b, H_c), 7.547 (t, H_d), 4.6128 (s, $2H_f$).

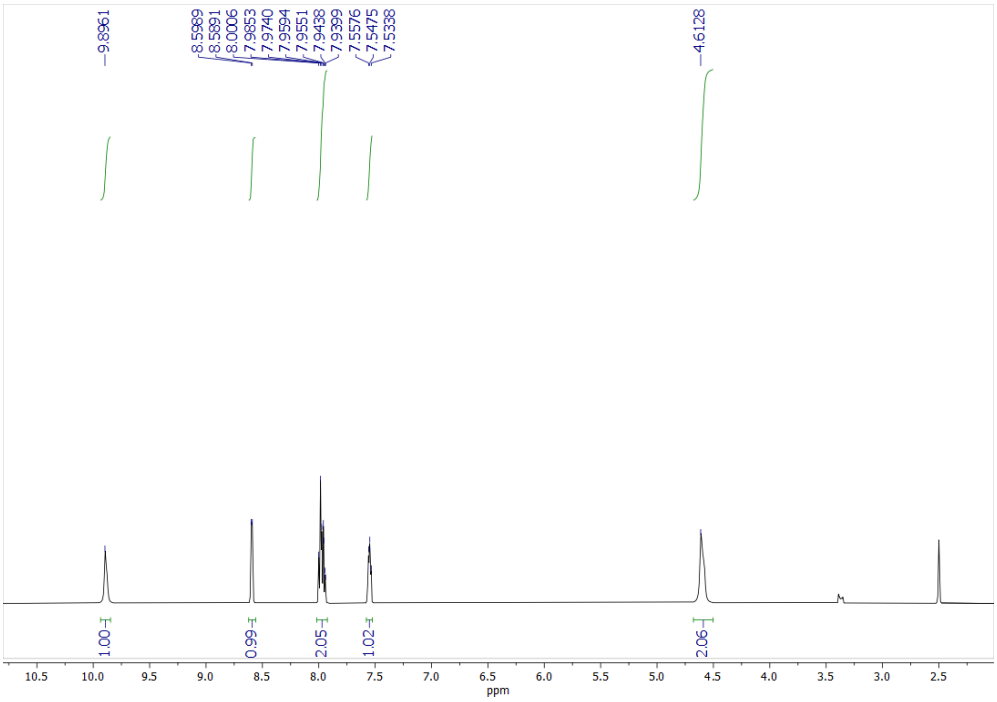

Synthesis of $[Yb_2(5\text{-Me-L})_2(DMF)_2(NO_3)_2]\cdot DMF$:

In 25 ml round bottom flask, a solution of picolinohydrazide (0.2 mmol, 28 mg) and 2-hydroxy-5-methylbenzaldehyde (0.2 mmol, 26 mg) in 6 ml mixed solvent (3 ml MeOH and 3 ml DMF) was stirred for 10 min in presence of few drops of (2-3 drops) glacial acetic acid. Then $Yb(NO_3)_3\cdot 6H_2O$ (0.2 mmol, 92 mg) and Et_3N (0.2 mmol) were added and refluxed the reaction mixture for 2 h. An intense yellow color solution and precipitate was obtained and cooled to room temperature. After filtration, the precipitate was dissolved in hot DMF and kept for crystallization by vapor diffusion with DEE at room temperature. The yellow color block shaped crystals suitable for X-ray crystallography are obtained after 2 days. (Yield 60%). Elem anal. Calcd for $C_{37}\ H_{42}\ N_{11}\ O_{13}\ Yb_2$: C, 37.19; H, 3.54; N, 12.89%. Found: C, 37.15; H, 3.49; N, 12.35%. IR (KBr pellet, 4000 − 400 cm^{-1}) ν /cm^{-1}: 3259, 2989, 2893, 2849, 2793, 1620, 1569, 1523, 1477, 1449, 1393, 1165, 1093, 810, 745.

Table S1. Crystal data and structure refinement for Complex **1**.

Identification code	**Complex** 1
Empirical formula	$C_{37}H_{42}N_{11}O_{13}Yb_2$
Formula weight	1194.89
Temperature/K	140
Crystal system	triclinic
Space group	P-1
a/Å	10.3127(6)
b/Å	10.4419(7)
c/Å	20.5492(13)
α/°	78.734(3)
β/°	80.248(3)

γ/°	83.810(3)
Volume/Å^3	2132.4(2)
Z	2
ρ_{calc}g/cm^3	1.861
μ/mm^{-1}	4.435
F(000)	1170.0
Crystal size/mm^3	0.73 × 0.57 × 0.49
Radiation	MoKα (λ = 0.71073)
2Θ range for data collection/°	2.044 to 51.72
Index ranges	-11 ≤ h ≤ 12, -12 ≤ k ≤ 11, -25 ≤ l ≤ 25
Reflections collected	28908
Independent reflections	8124 [R_{int} = 0.0282, R_{sigma} = 0.0333]
Data/restraints/parameters	8124/0/576
Goodness-of-fit on F^2	1.124
Final R indexes [I>=2σ (I)]	R_1 = 0.0249, wR_2 = 0.0470
Final R indexes [all data]	R_1 = 0.0299, wR_2 = 0.0592
Largest diff. peak/hole / e Å^{-3}	0.81/-1.03

Table S2. The SHAPE analysis for complexes **1**.

OP-8	1	D_{8h}	Octagon
HPY-8	2	C_{7v}	Heptagonal pyramid
HBPY-8	3	D_{6h}	Hexagonal bipyramid
CU-8	4	Oh	Cube
SAPR-8	5	D_{4d}	Square antiprism
TDD-8	6	D_{2d}	Triangular dodecahedron
JGBF-8	7	D_{2d}	Johnson gyrobifastigium J26
JETBPY-8	8	D_{3h}	Johnson elongated triangular bipyramid J14
JBTPR-8	9	C_{2v}	Biaugmented trigonal prism J50
BTPR-8	10	C_{2v}	Biaugmented trigonal prism
JSD-8	11	D_{2d}	Snub diphenoid J84
TT-8	12	Td	Triakis tetrahedron
ETBPY-8	13	D_{3h}	Elongated trigonal bipyramid

Structure ML_8	OP-8	HPY-8	HBPY-8	CU-8	SAPR-8	TDD-8	JGBF-8	JETBPY-8	JBTPR-8	BTPR-8	JSD-8	TT-8	ETBPY-8
1	31.464	20.456	17.023	14.617	5.222	3.735	13.387	24.141	3.377	**3.354**	5.052	15.019	22.528

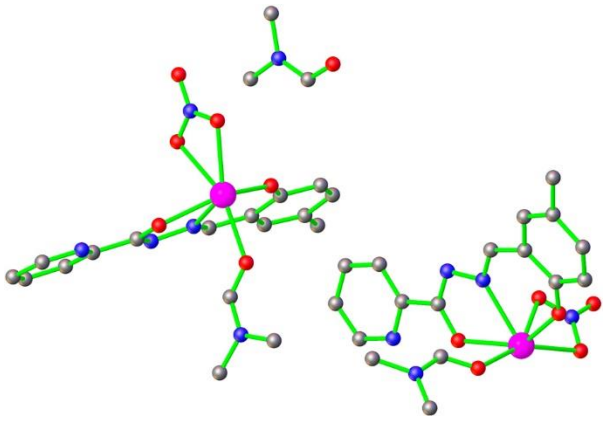

Fig S1. The asymmetric unit of complex **1**. Hydrogens are removed for clarity.

Table S3. Bond Lengths for Complex **1**.

Atom	Atom	Length/Å		Atom	Atom	Length/Å
Yb2	Yb2[1]	3.8083(4)		N2	C12	1.300(6)
Yb2	O8	2.296(3)		N11	C35	1.465(7)
Yb2	O7	2.117(3)		N11	C34	1.324(7)
Yb2	O9	2.255(3)		N11	C36	1.450(7)
Yb2	O9[1]	2.283(3)		N1	C8	1.285(6)
Yb2	O10	2.401(3)		N5	C9	1.311(6)
Yb2	O11	2.456(3)		N5	C11	1.457(6)
Yb2	N8[1]	2.488(4)		N5	C10	1.441(7)
Yb2	N6	2.432(4)		C8	C7	1.462(6)
Yb2	N10	2.857(4)		C30	C29	1.377(6)
Yb2	C28	3.143(4)		C30	C31	1.382(6)
Yb1	Yb1[2]	3.8333(4)		N3	C13	1.348(6)
Yb1	O3[2]	2.281(3)		N3	C17	1.355(6)
Yb1	O3	2.275(3)		C28	C29	1.485(6)
Yb1	O1	2.127(3)		N9	C27	1.457(6)
Yb1	O2	2.293(3)		N9	C25	1.310(6)
Yb1	N4	2.854(4)		N9	C26	1.458(6)
Yb1	O4	2.440(3)		O13	C34	1.218(6)
Yb1	O5	2.410(4)		C12	C13	1.470(6)
Yb1	N1	2.431(4)		C31	C32	1.378(7)
Yb1	N3[2]	2.491(3)		C1	C7	1.410(6)
Yb1	C12	3.151(4)		C1	C2	1.389(7)
Yb1	C9	3.206(5)		C32	C33	1.385(6)
O8	C25	1.245(5)		C24	C23	1.446(6)
O7	C18	1.327(5)		C13	C14	1.392(6)
O3	C12	1.322(5)		C23	C22	1.411(6)
O9	C28	1.327(5)		C23	C18	1.413(6)
O1	C1	1.330(5)		C7	C6	1.402(6)
O2	C9	1.252(5)		C6	C4	1.380(7)
O10	N10	1.280(5)		C14	C15	1.399(7)
N4	O4	1.272(5)		C17	C16	1.374(6)
N4	O5	1.258(5)		C2	C3	1.390(7)
N4	O6	1.219(5)		C22	C21	1.388(6)

O11	N10	1.267(5)		C18	C19	1.402(6)
O12	N10	1.220(5)		C21	C20	1.394(7)
N7	N6	1.425(5)		C21	C37	1.509(6)
N7	C28	1.293(5)		C19	C20	1.377(6)
N8	C29	1.357(6)		C15	C16	1.374(7)
N8	C33	1.341(5)		C4	C5	1.514(7)
N6	C24	1.292(5)		C4	C3	1.403(7)
N2	N1	1.418(5)				

Table S4. Bond Angles for complex **1**.

Table 5 Bond Angles for arp1_a.							
Atom	**Atom**	**Atom**	**Angle/°**	**Atom**	**Atom**	**Atom**	**Angle/°**
O8	Yb2	Yb2^{1}	80.56(8)	N3^{2}	Yb1	Yb1^{2}	98.38(8)
O8	Yb2	O10	152.99(11)	N3^{2}	Yb1	N4	97.50(12)
O8	Yb2	O11	153.79(11)	N3^{2}	Yb1	C12	151.55(12)
O8	Yb2	N8^{1}	83.62(11)	N3^{2}	Yb1	C9	101.91(12)
O8	Yb2	N6	83.31(11)	C12	Yb1	Yb1^{2}	54.04(9)
O8	Yb2	N10	176.54(11)	C12	Yb1	C9	66.69(12)
O8	Yb2	C28	84.47(11)	C9	Yb1	Yb1^{2}	74.39(9)
O7	Yb2	Yb2^{1}	170.62(8)	C25	O8	Yb2	128.7(3)
O7	Yb2	O8	91.06(11)	C18	O7	Yb2	141.1(3)
O7	Yb2	O9	141.76(11)	Yb1	O3	Yb1^{2}	114.60(12)
O7	Yb2	O9^{1}	150.42(11)	C12	O3	Yb1^{2}	125.3(3)
O7	Yb2	O10	94.23(12)	C12	O3	Yb1	120.0(3)
O7	Yb2	O11	91.41(12)	Yb2	O9	Yb2^{1}	114.08(12)
O7	Yb2	N8^{1}	84.32(12)	C28	O9	Yb2	120.4(3)
O7	Yb2	N6	75.91(11)	C28	O9	Yb2^{1}	125.5(3)
O7	Yb2	N10	92.40(11)	C1	O1	Yb1	140.0(3)
O7	Yb2	C28	120.81(11)	C9	O2	Yb1	127.0(3)
O9^{1}	Yb2	Yb2^{1}	32.73(7)	N10	O10	Yb2	97.1(2)
O9	Yb2	Yb2^{1}	33.19(7)	O4	N4	Yb1	58.3(2)
O9	Yb2	O8	82.20(11)	O5	N4	Yb1	56.9(2)
O9^{1}	Yb2	O8	81.98(11)	O5	N4	O4	115.2(4)
O9	Yb2	O9^{1}	65.92(12)	O6	N4	Yb1	178.1(3)
O9^{1}	Yb2	O10	80.40(11)	O6	N4	O4	122.5(4)
O9	Yb2	O10	108.68(11)	O6	N4	O5	122.3(4)
O9	Yb2	O11	79.79(11)	N10	O11	Yb2	94.9(3)
O9^{1}	Yb2	O11	107.43(11)	C28	N7	N6	110.1(4)
O9	Yb2	N8^{1}	131.61(11)	N4	O4	Yb1	95.3(3)
O9^{1}	Yb2	N8^{1}	66.40(11)	C29	N8	Yb2^{1}	117.3(3)
O9^{1}	Yb2	N6	131.05(11)	C33	N8	Yb2^{1}	125.8(3)
O9	Yb2	N6	65.95(11)	C33	N8	C29	116.6(4)
O9^{1}	Yb2	N10	94.93(11)	N7	N6	Yb2	117.5(2)
O9	Yb2	N10	95.13(11)	C24	N6	Yb2	130.0(3)
O9	Yb2	C28	21.34(11)	C24	N6	N7	112.1(4)
O9^{1}	Yb2	C28	87.26(11)	C12	N2	N1	110.3(4)
O10	Yb2	Yb2^{1}	95.15(9)	N4	O5	Yb1	97.2(3)
O10	Yb2	O11	52.60(11)	O10	N10	Yb2	56.5(2)
O10	Yb2	N8^{1}	70.62(11)	O11	N10	Yb2	58.9(2)
O10	Yb2	N6	123.66(11)	O11	N10	O10	115.3(4)
O10	Yb2	N10	26.40(11)	O12	N10	Yb2	176.6(3)
O10	Yb2	C28	114.83(11)	O12	N10	O10	122.3(4)

O11	Yb2	Yb2[1]	94.28(8)		O12	N10	O11	122.3(4)
O11	Yb2	N8[1]	122.58(12)		C34	N11	C35	122.6(4)
O11	Yb2	N10	26.21(11)		C34	N11	C36	121.7(5)
O11	Yb2	C28	71.93(11)		C36	N11	C35	115.6(5)
N8[1]	Yb2	Yb2[1]	98.81(8)		N2	N1	Yb1	117.7(3)
N8[1]	Yb2	N10	96.60(12)		C8	N1	Yb1	129.7(3)
N8[1]	Yb2	C28	152.33(11)		C8	N1	N2	112.5(4)
N6	Yb2	Yb2[1]	98.77(8)		C9	N5	C11	121.1(4)
N6	Yb2	O11	72.04(11)		C9	N5	C10	121.3(5)
N6	Yb2	N8[1]	156.02(11)		C10	N5	C11	117.6(4)
N6	Yb2	N10	97.65(12)		N1	C8	C7	125.6(4)
N6	Yb2	C28	44.92(11)		C29	C30	C31	118.6(4)
N10	Yb2	Yb2[1]	96.00(7)		C13	N3	Yb1[2]	117.6(3)
N10	Yb2	C28	93.85(11)		C13	N3	C17	117.5(4)
C28	Yb2	Yb2[1]	54.53(8)		C17	N3	Yb1[2]	124.8(3)
O3[2]	Yb1	Yb1[2]	32.65(7)		O9	C28	Yb2	38.21(18)
O3	Yb1	Yb1[2]	32.75(8)		O9	C28	C29	115.2(4)
O3	Yb1	O3[2]	65.40(12)		N7	C28	Yb2	87.1(3)
O3[2]	Yb1	O2	83.64(12)		N7	C28	O9	125.0(4)
O3	Yb1	O2	82.07(11)		N7	C28	C29	119.8(4)
O3	Yb1	N4	95.13(11)		C29	C28	Yb2	152.6(3)
O3[2]	Yb1	N4	95.19(12)		C27	N9	C26	117.1(4)
O3[2]	Yb1	O4	83.43(12)		C25	N9	C27	121.5(4)
O3	Yb1	O4	111.15(12)		C25	N9	C26	121.5(4)
O3	Yb1	O5	78.12(12)		N8	C29	C30	123.2(4)
O3[2]	Yb1	O5	105.22(13)		N8	C29	C28	114.7(4)
O3	Yb1	N1	65.62(12)		C30	C29	C28	122.1(4)
O3[2]	Yb1	N1	130.12(11)		O3	C12	Yb1	38.7(2)
O3[2]	Yb1	N3[2]	66.10(11)		O3	C12	C13	115.9(4)
O3	Yb1	N3[2]	130.69(11)		N2	C12	Yb1	86.5(3)
O3[2]	Yb1	C12	86.69(12)		N2	C12	O3	124.5(4)
O3	Yb1	C12	21.30(12)		N2	C12	C13	119.6(4)
O3[2]	Yb1	C9	86.51(12)		C13	C12	Yb1	153.3(3)
O3	Yb1	C9	66.89(12)		C32	C31	C30	119.7(5)
O1	Yb1	Yb1[2]	169.13(8)		O1	C1	C7	122.8(4)
O1	Yb1	O3[2]	150.55(11)		O1	C1	C2	119.4(4)
O1	Yb1	O3	141.44(11)		C2	C1	C7	117.7(4)
O1	Yb1	O2	88.57(12)		C31	C32	C33	118.0(4)
O1	Yb1	N4	93.67(12)		N6	C24	C23	125.2(4)
O1	Yb1	O4	92.46(12)		N3	C13	C12	114.5(4)
O1	Yb1	O5	94.84(13)		N3	C13	C14	123.0(4)
O1	Yb1	N1	76.01(12)		C14	C13	C12	122.5(4)
O1	Yb1	N3[2]	84.93(12)		C22	C23	C24	117.0(4)
O1	Yb1	C12	120.86(12)		C22	C23	C18	119.4(4)
O1	Yb1	C9	94.82(12)		C18	C23	C24	123.7(4)
O2	Yb1	Yb1[2]	81.50(8)		C1	C7	C8	123.6(4)
O2	Yb1	N4	177.20(11)		C6	C7	C8	116.2(4)
O2	Yb1	O4	155.33(11)		C6	C7	C1	120.1(4)
O2	Yb1	O5	152.18(11)		C4	C6	C7	122.0(4)
O2	Yb1	N1	80.99(12)		N8	C33	C32	124.0(4)
O2	Yb1	N3[2]	84.36(11)		O2	C9	Yb1	34.9(2)
O2	Yb1	C12	84.52(11)		O2	C9	N5	124.6(5)
O2	Yb1	C9	18.19(11)		N5	C9	Yb1	158.9(4)

N4	Yb1	Yb1^{2}	96.14(8)		C13	C14	C15	117.9(4)
N4	Yb1	C12	92.88(11)		N3	C17	C16	122.8(5)
N4	Yb1	C9	159.41(12)		C1	C2	C3	121.4(5)
O4	Yb1	Yb1^{2}	98.40(9)		C21	C22	C23	122.5(4)
O4	Yb1	N4	26.33(11)		O8	C25	N9	125.8(4)
O4	Yb1	N3^{2}	71.20(12)		O7	C18	C23	123.4(4)
O4	Yb1	C12	115.55(12)		O7	C18	C19	119.5(4)
O4	Yb1	C9	169.50(13)		C19	C18	C23	117.1(4)
O5	Yb1	Yb1^{2}	91.96(10)		C22	C21	C20	117.3(4)
O5	Yb1	N4	25.93(11)		C22	C21	C37	121.4(4)
O5	Yb1	O4	52.25(12)		C20	C21	C37	121.2(4)
O5	Yb1	N1	73.14(12)		C20	C19	C18	122.5(4)
O5	Yb1	N3^{2}	123.42(12)		C16	C15	C14	119.3(4)
O5	Yb1	C12	70.03(11)		C6	C4	C5	121.9(4)
O5	Yb1	C9	134.27(12)		C6	C4	C3	117.5(5)
N1	Yb1	Yb1^{2}	97.96(9)		C3	C4	C5	120.6(5)
N1	Yb1	N4	97.91(12)		C2	C3	C4	121.2(5)
N1	Yb1	O4	123.14(12)		C19	C20	C21	121.1(4)
N1	Yb1	N3^{2}	156.14(12)		C15	C16	C17	119.5(5)
N1	Yb1	C12	44.88(13)		O13	C34	N11	125.8(5)
N1	Yb1	C9	66.18(12)					

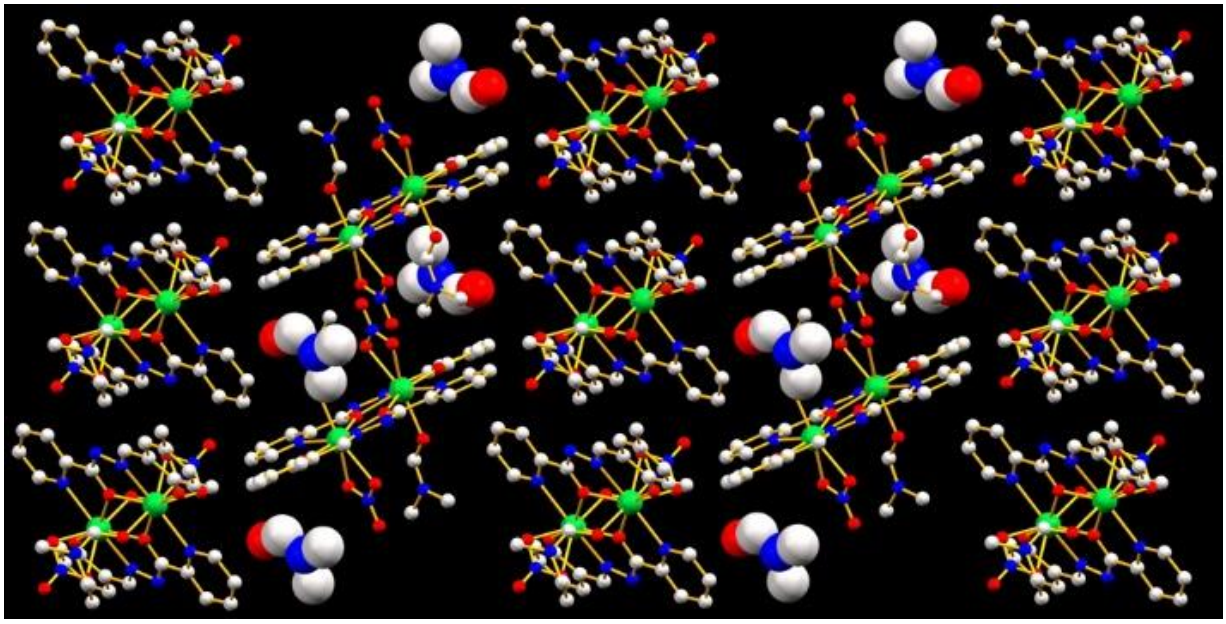

Fig S2. Presence of solvent molecules and 2D supramolecular arrangement of complex **1** along crystallographic *b* axis.

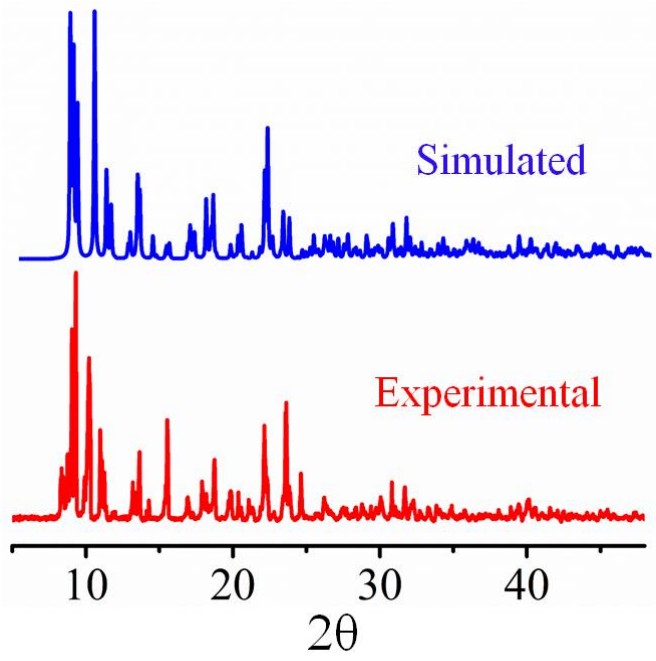

Fig S3. Simulated patters for single crystal and Powder-XRD for bulk sample of complex **1**.

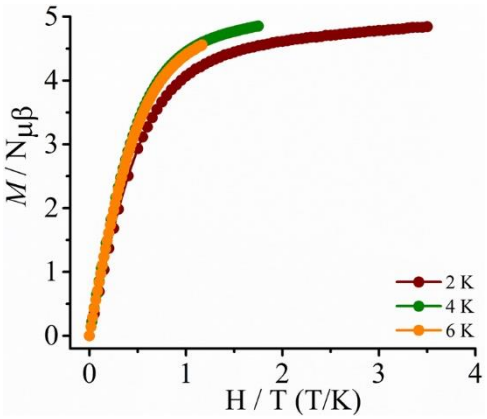

Fig S4. Reduced magnetization plot at the indicated temperature for complex **1.**

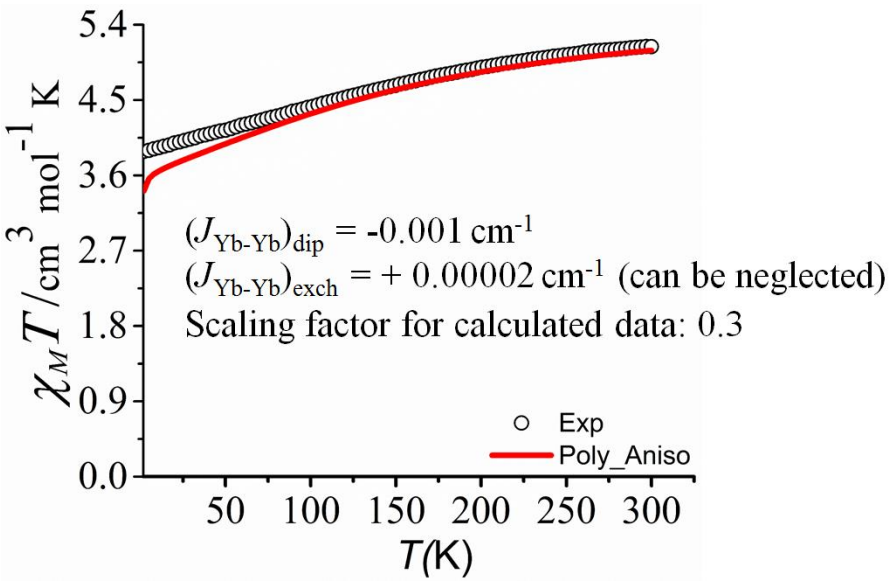

Fig S5. The fits of experimental magnetic susceptibility of **1** utilizing POLY_ANISO module**.**

BS-DFT Calculations

To gain insight into the magnetic exchange coupling between the Yb centres, the BS-DFT calculations were performed by replacing Yb^{+3} with isotropic Gd^{+3} ions within the ORCA 4.0 software package.[1] The relativistic effects were included with the zero order regular approximation (ZORA), together with the scalar relativistic contracted version of the basis functions def2-TZVPP for Gd, and def2-TZVP(-f) for N, O, C and H atoms. In these calculations the well-known B3LYP functional was employed to extract the isotropic exchange coupling using the method of Yamaguchi where the exchange coupling is determined from the energies (E) and expectation values ($<S^2>$) of the triplet and broken symmetry singlet states. Later the obtained isotropic exchange coupling constant *J* has been rescaled to the pseudo spin ½ of the corresponding lanthanide atoms.

$$J = \frac{-(E_T - E_{BSS})}{<S^2>_T - <S^2>_{BSS}}$$

Energy of the high spin and broken symmetry state for **1**			Exchange coupling constant (cm^{-1})
Spin State	Energy (Hatree)	$<S^2>$	-0.007 (Yb-Yb)
HS	-25814.654911	56.0121	
BS	-25814.654922	7.0121	

Simulation of Molar Magnetic Susceptibility and Magnetization

To simulate the direct current magnetic susceptibility and magnetization data, we have performed simulation in PHI using lines' model. The SHAPE analysis shows that the ytterbium

center possess C_{2V} point group in the studied complex. Therefore, we have used following Hamiltonian to simulate the direct current magnetic susceptibility and magnetization data.

$$\hat{H}_{CF} = -2J_{Yb\text{-}Yb}\,(S_{Yb1}\cdot S_{Yb2}) + B_0^2C_0^2 + B_2^2C_2^2 + B_0^4C_0^4 + B_2^4C_2^4 + B_4^4C_4^4 + B_0^6C_0^6 + B_2^6C_2^6 + B_4^6C_4^6 + B_6^6C_6^6$$

Where B_q^k is the crystal field parameter, J (J_{exch} + J_{dip}) is the exchange coupling constant between ytterbium center, C_q^k is the crystal field matrix. In this regard, we have used the crystal field parameters obtained from the ab initio calculation, and exchange coupling constant J obtained from BS-DFT calculations during the simulation. It was found that the parameters obtained from theoretical calculations (CFPs and J) replicate both the magnetic susceptibility as well as magnetization data for the studied complexes. However, a little discrepancy between the simulated and experimental data are commonly observed as reported in the literature.[9] Further, the simulation of the excited states reveals that first four exchange coupled states are almost degenarate and the siginificant energy difference is observed at 314 cm^{-1} which is very close to the energy difference between ground and excited states (306 cm^{-1}) obtained from Single_Aniso calculations (vide infra).

Table S5. The energy of the exchange coupled states and Single_Aniso computed KDs for the studied complex.

Energy of the Exchange coupled states	Energy of the KDs obtained from Single_Aniso calculation
0.000	0.000
314.79	306.350
518.81	522.631
629.59	663.14

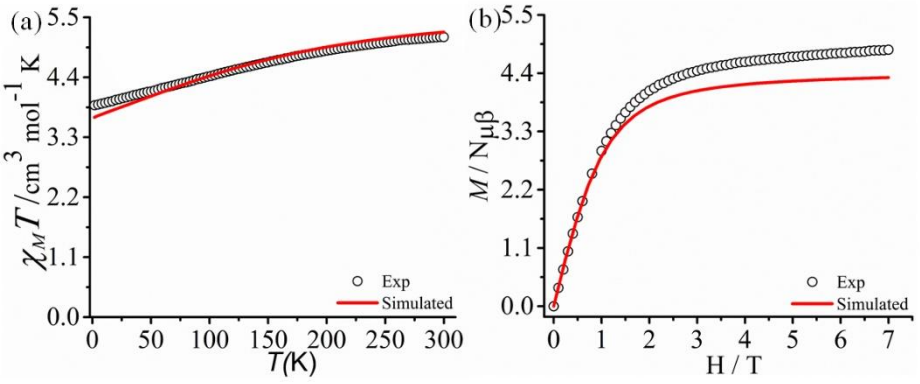

Fig S6. Experimental and simulated magnetic data using lines model obtained from BS-DFT calculated exchange coupling constant and ab initio calculations.

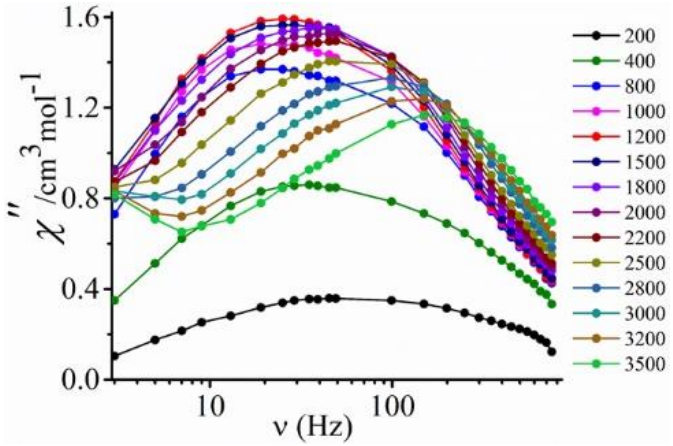

Fig S7. The out-of-phase (χ′′) susceptibility under different external magnetic fields (Oe) at 2 K and the highest peak maxima observed under 1200 Oe field (Optimum field). The additional peaks at higher magnetic fields (above 2200 Oe) may be due to the presence of direct process.

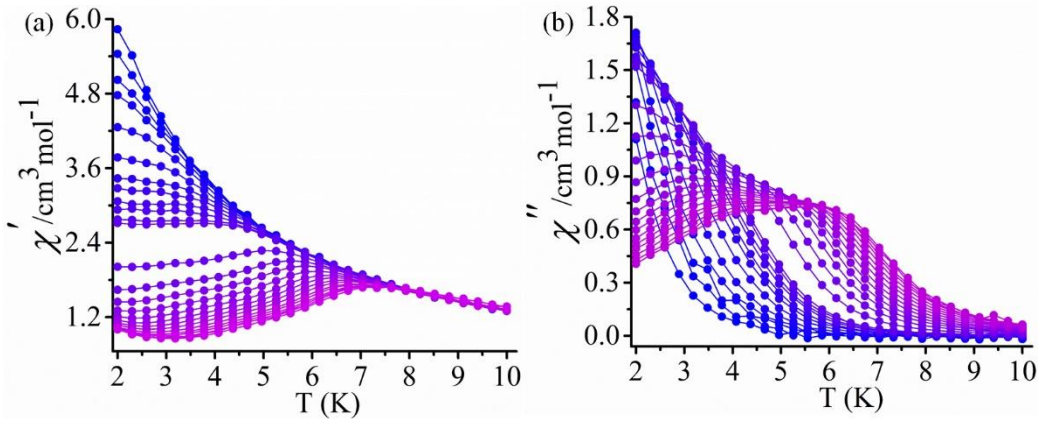

Fig S8. Temperature dependence of in-phase (χ′) (a) and out-of-phase (χ′′) (b) susceptibility collected under 0.12 T external dc field in the range of frequency 1-750 Hz.

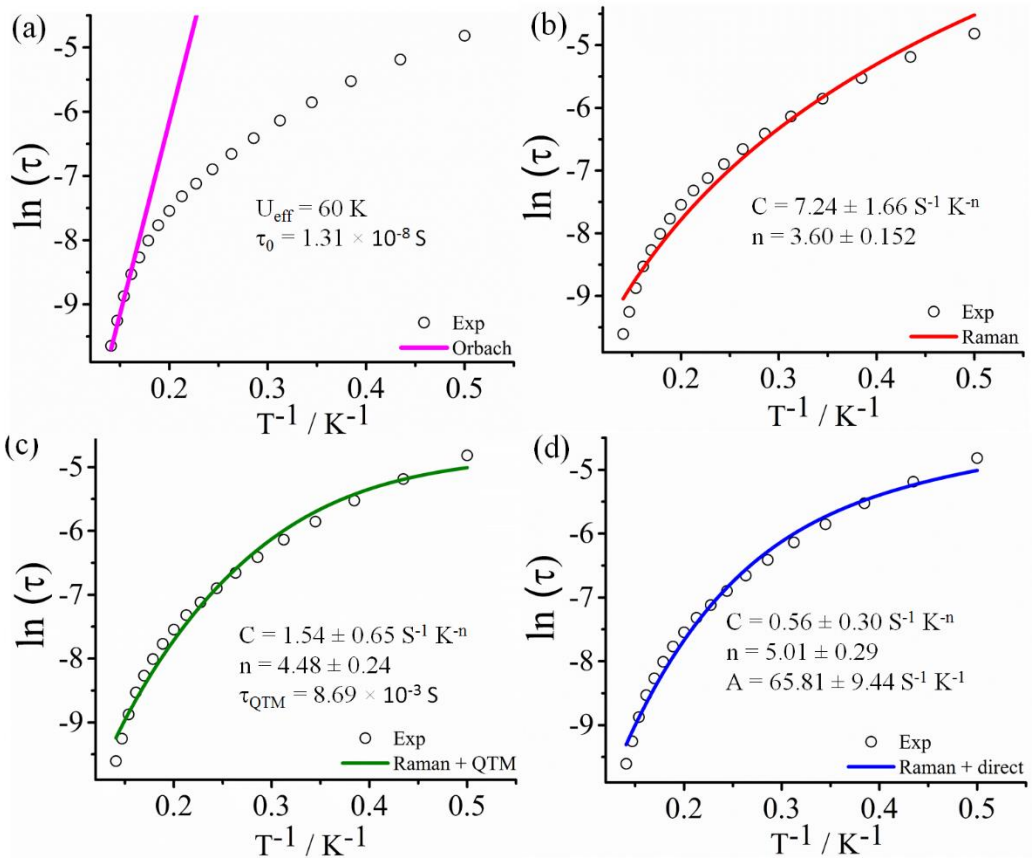

Fig S9. The fitting of temperature dependence of relaxation time with different combinations of relaxation process.

Table S6. The parameters obtained from the fitting of frequency dependent data using generalized Debye model for complex **1**.

T (K)	χ_S	χ_T	τ (s)	α
2	0.60882	6.93762	0.00809 ($\pm 1.96 \times 10^{-4}$)	0.3629
2.3	0.53493	6.06814	0.00558 ($\pm 1.10 \times 10^{-4}$)	0.34426
2.6	0.47826	5.36561	0.00399 ($\pm 6.64 \times 10^{-5}$)	0.32838
2.9	0.44837	4.77449	0.00287 ($\pm 5.64 \times 10^{-5}$)	0.30977
3.2	0.43268	4.33001	0.00216 ($\pm 4.91 \times 10^{-5}$)	0.29582
3.5	0.41108	3.9459	0.00164 ($\pm 4.23 \times 10^{-5}$)	0.28639
3.8	0.42514	3.631	0.00128 ($\pm 3.55 \times 10^{-5}$)	0.27077
4.1	0.43767	3.34746	0.00101 ($\pm 2.88 \times 10^{-5}$)	0.25595
4.4	0.4857	3.09339	8.09×10^{-4} ($\pm 2.41 \times 10^{-5}$)	0.22821
4.7	0.53844	2.88616	6.63×10^{-4} ($\pm 2.09 \times 10^{-5}$)	0.19835
5	0.56937	2.68423	5.28×10^{-4} ($\pm 1.67 \times 10^{-5}$)	0.16307
5.3	0.58658	2.52312	4.23×10^{-4} ($\pm 1.30 \times 10^{-5}$)	0.13441
5.6	0.59022	2.38362	3.32×10^{-4} ($\pm 1.01 \times 10^{-5}$)	0.10899
5.9	0.57243	2.25313	2.56×10^{-4} ($\pm 8.11 \times 10^{-6}$)	0.08376

6.2	0.50806	2.13255	1.97×10^{-4} ($\pm 8.01 \times 10^{-6}$)	0.06881
6.5	0.42727	2.04864	1.39×10^{-4} ($\pm 6.01 \times 10^{-6}$)	0.07071
6.8	0.36642	1.95161	9.57×10^{-5} ($\pm 5.64 \times 10^{-6}$)	0.07423
7.1	0	1.86829	6.27×10^{-5} ($\pm 7.59 \times 10^{-7}$)	0.06255

Table S7. Comparison of U_{eff} value of this work with the other reported Yb-based SMMs.

SL. No.	Complex	H_{dc}(Oe)	U_{eff} (K)	τ_0(s)	Ref.
1	$[Yb(Ph_3PO)_4(OTf)_2][OTf]\cdot(C_2H_5OH)_{0.5}$	2000	28 (Orbach)	2.88×10^{-8}	9b
2	$[Yb_2(valdien)_2(NO_3)_2]$ H_2valdien = N1,N3-bis(3-methoxysalicylidene)diethylenetriamine	1000	66 (Orbach + Raman+ QTM)	4.62×10^{-8}	9c
3	$[YbL(NO_3)_3(MeOH)]\cdot MeCN$ L = (2-(1-methyl-2-((1- methyl-1H-imidazol-2-yl)methylene)hydrazinyl)pyridine)	1000	17.8 (Orbach)	8.7×10^{-7}	10a
4	$[YbZn_4(quinha)_4(iqn)_4(DMF)_4](CF_3SO_3)_3\cdot 6DMF\cdot 4H_2O$ [Hquinha = quinaldichydroxamic acid, iqn = isoquinoline]	600	22.76 (Orbach)	3.90×10^{-7}	10b
5	$[Yb(H_3Bmshp)(DMF)_2Cl_2]\cdot DMF\cdot 1.5H_2O$ $[Yb(H_3Bmshp)(DMF)_2Cl_2]\cdot H_4Bmshp$ H_4Bmshp = (2,6-bis[(3-ethoxysalicylidene) hydrazinecarbonyl]-pyridine)	1500 600	14.5 (Orbach) 38.3 (Orbach)	2.38×10^{-5} 7.16×10^{-7}	10c
6	Yb(trensal), H_3trensal=2,2′,2″-tris(salicylideneimino)triethylamine	2000	53.2 (Orbach)	1.51×10^{-8}	10d
7	$[Yb(H_2O)_5(NCS)_3]\cdot H_2O$	2500	50 (Orbach)	2.3×10^{-8}	10e
8	$[Yb_2(5\text{-Me-L})_2(DMF)_2(NO_3)_2]\cdot DMF$ L = 5-Me-LH_2 = N'-(2-hydroxy-5-methylbenzylidene)picolinohydrazide	1200	60 (Orbach) 77.1 (Orbach + Raman)	1.33×10^{-8} 1.70×10^{-9}	This work

Table S8. SINGLE_ANISO computed crystal-field parameters for complex **1**.

k	Q	Complex **1**
	-2	-0.1374E+01
	-1	-0.2748E+01
2	0	-0.1211E+02
	1	0.3086E+01
	2	0.1901E+02
	$\lvert B_2^2/B_2^0 \rvert$ [only B_2^2	1.56

	is considered as it has larger contribution]	
	-4	0.9570E-01
	-3	0.2706E+00
	-2	0.7234E-01
	-1	0.1023E+00
4	0	-0.1503E+00
	1	-0.8369E-01
	2	0.3305E+00
	3	0.3752E-01
	4	-0.2868E+00
	-6	0.3474E-01
	-5	0.1203E+00
	-4	0.2565E-01
	-3	0.4684E-01
	-2	0.2342E-01
	-1	0.2962E-01
6	0	-0.2025E-02
	1	0.6881E-02
	2	-0.1005E-02
	3	0.7402E-02
	4	-0.3483E-02
	5	0.1014E-01
	6	0.4246E-01

Table S9. Ab initio calculated low-lying spin-free and spin-orbit energy states for the investigated complex.

Spin-free energy states	Spin-orbit energy states
0.000	0.000
274.907	306.350
411.917	306.350
574.470	522.631
702.038	522.631
745.839	663.148
860.084	663.148

Table S10. Single_Aniso computed energy of the KDs, g and wavefuctions composition for Complex **1**.

Kramers doublets (KDs)	Energy (cm^{-1})	g_x	g_y	g_z	angle (°)	Wave function composition
1	0.000	0.821	1.762	7.01		86.67%|±7/2>+8.37%|±3/2>+ 2.55%|±5/2>+2.39%|±1/2>
2	306.35	1.326	2.520	4.707	78.18	42.82%|±1/2>+36.74%|±5/2> +11.49%|±3/2>+8.39%|±7/2>
3	522.63	0.033	2.319	5.219	81.55	56.45%|±3/2>+34.52%|±5/2> +5.96%|±1/2>+3.04%|±7/2>
4	663.14	0.782	1.183	7.409	98.24	48.80%|±1/2>+26.17%|±5/2> +23.67%|±3/2>+1.34%|±7/2>

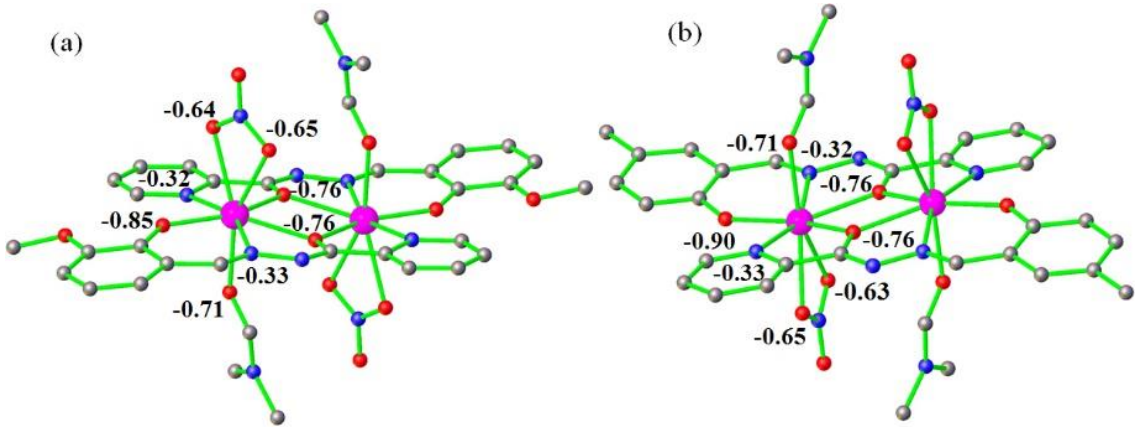

Fig S10. LoProp charges of the selected atoms for the reported dinuclear ytterbium analogue (a) and studied complex (b).

Table S11. Energy of the four KDs and corresponding g tensor for model complex **1a**.

Energy (cm^{-1})	g_x	g_y	g_z
0.0	0.642	1.195	7.35
427.5	1.429	2.231	5.47
784.0	1.190	1.818	5.28
1139.2	0.386	0.436	7.83

Table S12. Energy of the four KDs and corresponding g tensor for model complex **1b**.

Energy (cm^{-1})	g_x	g_y	g_z
0.0	0.31	0.38	7.87
1132.5	0.78	1.47	5.23
1694.5	2.33	2.53	3.95
2217.5	0.38	0.725	7.52

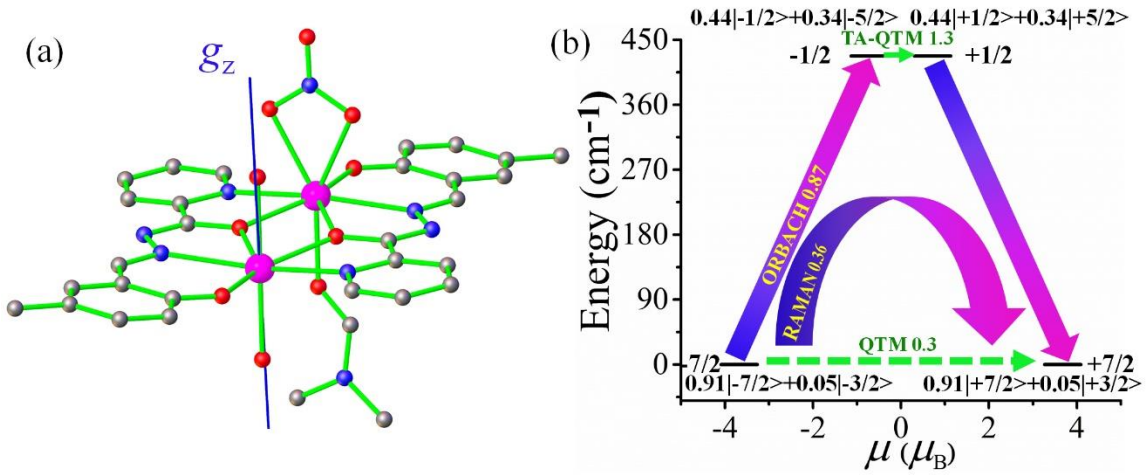

Fig S11. The orientation of the anisotropic axis for the ground state (a) and calculated blockade barrier for model complex **1a**. The values provided at each arrow represent the corresponding matrix element of the transition magnetic moment.

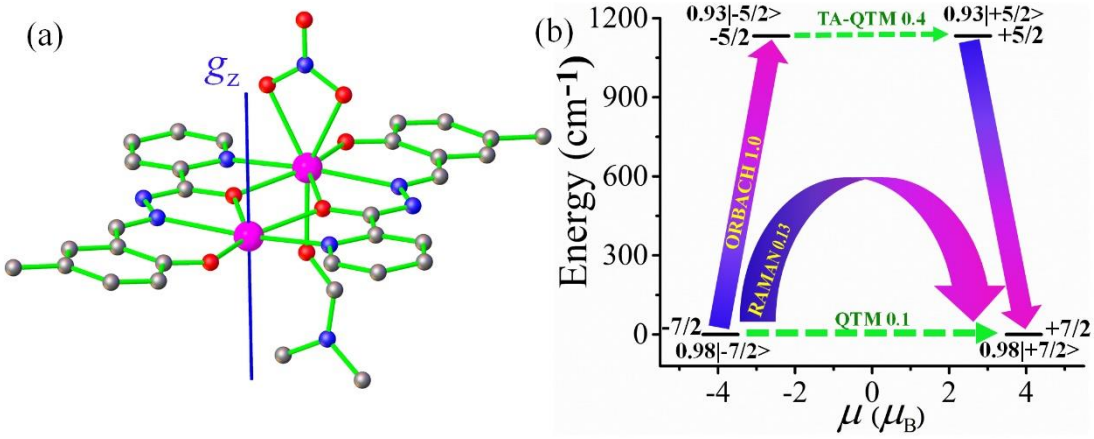

Fig S12. The orientation of the anisotropic axis for the ground state (a) and calculated blockade barrier for model complex **1b**. The values provided at each arrow represent the corresponding matrix element of the transition magnetic moment.

Reference:

1. Kahn, O. *Molecular Magnetism*, VCH Publishers Inc. **1991**.
2. G. Sheldrick, *Acta Crystallogr C.*, 2015, **71**, 3.
3. O. V. Dolomanov, L. J. Bourhis, R. J. Gildea, J. A. K. Howard and H. Puschmann, *J. Appl. Crystallogr.*, 2009, **42**, 339-341.
4. 4. F. Aquilante, J. Autschbach, R. K. Carlson, L. F. Chibotaru, M. G. Delcey, L. De Vico, I. Fdez. Galván, N. Ferré, L. M. Frutos, L. Gagliardi, M. Garavelli, A. Giussani, C. E.

Hoyer, G. Li Manni, H. Lischka, D. Ma, P. Å. Malmqvist, T. Müller, A. Nenov, M. Olivucci, T. B. Pedersen, D. Peng, F. Plasser, B. Pritchard, M. Reiher, I. Rivalta, I. Schapiro, J. Segarra-Martí, M. Stenrup, D. G. Truhlar, L. Ungur, A. Valentini, S. Vancoillie, V. Veryazov, V. P. Vysotskiy, O. Weingart, F. Zapata and R. Lindh, J. Comput. Chem., 2016, **37**, 506.

5. B. A. Heß, C. M. Marian, U. Wahlgren and O. Gropen, *Chem. Phys. Lett.*, 1996, **251**, 365-371.
6. B. O. Roos and P.-Å. Malmqvist, *PCCP*, 2004, **6**, 2919-2927.
7. P. Å. Malmqvist, B. O. Roos and B. Schimmelpfennig, *Chem. Phys. Lett.*, 2002, **357**, 230-240.
8. L. F. Chibotaru and L. Ungur, *J. Chem. Phys.*, 2012, **137**, 064112.
9. (a) M. J. Giansiracusa, S. Al-Badran, A. K. Kostopoulos, G. F. S. Whitehead, E. J. L. McInnes, D. Collison, R. E. P. Winpenny and N. F. Chilton, *Inorg. Chem. Front.*, 2020, **7**, 3909-3918. (b) A. Borah, S. Dey, S. K. Gupta, M. G. Walawalkar, G. Rajaraman and R. Murugavel, *Chem. Commun.*, 2020, **56**, 11879-11882. (c) G. Brunet, R. Marin, M.-J. Monk, U. Resch-Genger, D. A. Gálico, F. A. Sigoli, E. A. Suturina, E. Hemmer and M. Murugesu, *Chem. Sci.*, 2019, **10**, 6799-6808.
10. (a) A. Gorczyński, D. Marcinkowski, M. Kubicki, M. Löffler, M. Korabik, M. Karbowiak, P. Wiśniewski, C. Rudowicz and V. Patroniak, *Inorg. Chem. Front.*, 2018, **5**, 605-618. (b) Q.-W. Li, J.-L. Liu, J.-H. Jia, Y.-C. Chen, J. Liu, L.-F. Wang and M.-L. Tong, *Chem. Commun.*, 2015, **51**, 10291-10294. (c) D.-Q. Wu, D. Shao, X.-Q. Wei, F.-X. Shen, L. Shi, Y.-Q. Zhang and X.-Y. Wang, *Dalton Trans.*, 2017, **46**, 12884-12892. (d) K. S. Pedersen, J. Dreiser, H. Weihe, R. Sibille, H. V. Johannesen, M. A. Sørensen, B. E. Nielsen, M. Sigrist, H. Mutka, S. Rols, J. Bendix and S. Piligkos, *Inorg. Chem.*, 2015, **54**, 7600-7606. (e) S. P. Petrosyants, K. A. Babeshkin, A. V. Gavrikov, A. B. Ilyukhin, E. V. Belova and N. N. Efimov, *Dalton Trans.*, 2019, **48**, 12644-12655.